Secondary Structure of the Exchange-Resistant Core from the Nicotinic Acetylcholine Receptor Probed Directly by Infrared Spectroscopy and Hydrogen/Deuterium Exchange†

Nathalie Méthot and John E. Baenziger*

Department of Biochemistry, University of Ottawa, Ottawa, Ontario, K1H 8M5, Canada

Received April 15, 1998; Revised Manuscript Received August 7, 1998

ABSTRACT: The spectral changes that occur in infrared spectra recorded as a function of time after exposure of the nicotinic acetylcholine receptor (nAChR) to ^2H_2O buffer were examined in order to investigate the secondary structure of the transmembrane domain. The resolution-enhanced amide I band in spectra recorded during the first 12 h after exposure to ^2H_2O exhibits subtle downshifts in frequency of α-helical and β-sheet vibrations. A strong intensity of the unexchanged α-helical vibration near 1655 cm^{-1} after 3 days exposure to ^2H_2O suggests that a large proportion of the remaining 25% of unexchanged peptide hydrogens adopts an α-helical conformation. Further exposure of the nAChR to ^2H_2O under conditions of both increasing pH and membrane "fluidity" led to additional exchange of peptide hydrogens for deuterium. The greatest degree of peptide $^1H/^2H$ exchange (95%) under nondenaturing conditions was found for the nAChR reconstituted into the highly fluid egg phosphatidylcholine membranes lacking cholesterol and anionic lipids at pH 9.0. This enhanced exchange was accompanied by a decrease in intensity near 1655 cm^{-1} due to the downshift in frequency of peptides in the α-helical conformation, whereas no clear evidence was found for the further exchange of β-sheet. Some unexchanged α-helical peptide hydrogens were still observed. As the exchange-resistant peptides likely include those found within the hydrophobic environment of the lipid bilayer, these data strongly support an α-helical secondary structure of the transmembrane domain.

The nicotinic acetylcholine receptor (nAChR)[1] from the electric organ of *Torpedo* is the most intensively studied member of a family of ligand-gated ion channels that performs a key role in synaptic transmission throughout the central and peripheral nervous systems (for reviews, see *1*, *2*). The *Torpedo* nAChR responds to the binding of the neurotransmitter acetylcholine by transiently opening a cation-selective ion channel across the postsynaptic membrane. Prolonged exposure to agonist as well as to a wide variety of noncompetitive antagonists leads to the formation of a channel-inactive desensitized state. The nAChR is a large integral membrane protein (∼300 000 daltons) composed of four distinct subunits arranged as an $\alpha_2\beta\gamma\delta$ pentamer around a central ion channel pore. The four subunits exhibit a high degree of homology including four conserved ∼25 amino acid residue long hydrophobic stretches designated M1−M4 (*3*, *4*). Five transmembrane M2 segments, one from each subunit, line the ion channel and control channel selectivity (*5*, *6*). M2 in conjunction with the transmembrane segments M1, M3, and M4 likely performs an important role in channel gating and desensitization (*7*−*9*, *23*).

An accurate structural model of the transmembrane domain is clearly required for a detailed understanding of the mechanisms of nAChR function. In the absence of high-resolution structural information, however, even the secondary structures of the transmembrane segments remain controversial. Each of the four hydrophobic transmembrane segments M1−M4 was originally assigned an α-helical secondary structure in analogy to the α-helical transmembrane segments that had been identified in other integral membrane proteins, such as bacteriorhodopsin (*10*). In agreement with this structural model, a number of site-directed mutagenesis and photoaffinity labeling experiments suggest an α-helical exposure of the transmembrane M2 segment to the ion channel pore (*11*−*14*). Five cylindrical rods of electron density consistent with α-helical M2 segments lining the ion channel are observed in a 9 Å resolution electron density map of the nAChR (*15*). NMR and CD analysis of synthetic M2 transmembrane peptides are also consistent with an α-helical secondary structure (*16*, *17*).

While a consensus has been reached with respect to the secondary structure of M2, conflicting experimental evidence has accumulated regarding the secondary structures of M1, M3, and M4. Both M3 and M4 exhibit an α-helical periodicity in their exposure to the lipid bilayer as monitored using photoactivatable hydrophobic probes (*18*, *19*). The

† This work was supported by a grant from the Medical Council of Canada to J.E.B. and by a doctoral scholarship from the Natural Sciences and Engineering Research Council to N.M.

* To whom correspondence should be addressed.

[1] Abbreviations: ATR, attenuated total reflectance; EPC, egg phosphatidylcholine; DOPA, dioleoylphosphatidic acid; FTIR, Fourier transform infrared; nAChR, nicotinic acetylcholine receptor; T_m, melting temperature.

10.1021/bi980848o CCC: $15.00
Published on Web 10/01/1998

labeling pattern of M1 by the same hydrophobic probes is consistent with a distorted α-helix, possibly due to the presence of an α-helix-breaking proline residue. Purified and reconstituted proteolytic fragments of M1, M3, and M4 show a strong propensity to adopt an α-helical secondary structure (*20*). In contrast, the lack of well-defined rods of electron density in regions of the nAChR peripheral to the ion channel pore in the 9 Å resolution electron density map has led to the suggestion that M1, M3, and M4 collectively form either five or seven transmembrane β-strands (*15*). Both FTIR spectra of the nAChR treated with proteinase-K to remove the extramembranous domains and molecular modeling studies have also suggested a mixed α/β secondary structure for the transmembrane domain of the nAChR (*21*, *22*).

We recently showed that FTIR spectra recorded after exposure of the nAChR to ^2H_2O exhibit changes in the shape of the secondary structure sensitive amide I band that result from the downshifts in frequency of α-helix and β-sheet amide I component bands (*24*). We also showed that roughly 25% of the nAChR peptide hydrogens remain in the protiated form after 3 days exposure to ^2H_2O at 4 °C. Here, we have examined nondenaturing alkaline conditions that lead to the exchange of most of the 25% "exchange resistant" peptide hydrogens in the nAChR. A careful analysis of spectra recorded over the time course of this enhanced peptide $^1H/^2H$ exchange reveals a downshift in frequency of the α-helical amide I component band, confirming that there are a substantial number of exchange-resistant α-helical peptide hydrogens in the nAChR. In contrast, the vibrational frequency of the main β-sheet amide I component band is essentially unaffected by the enhanced peptide $^1H/^2H$ exchange, suggesting that there are few, if any, exchange-resistant β-strands. Given that the 25% exchange-resistant peptide hydrogens likely include those found within the transmembrane domains, our results suggest an essentially α-helical secondary structure for M1−M4.

MATERIALS AND METHODS

Sample Preparation. The nAChR from frozen electric tissue of *Torpedo californica* (Marinus, Long Beach, CA) was affinity purified on a bromoacetylcholine bromide-derivatized Bio-Rad Affi-gel 102 column (Richmond, CA) as described previously (*25*, *26*). The affinity-purified nAChR was reconstituted into membranes composed of either soybean asolectin (type II-S) from Sigma (St. Louis, MO) or egg phosphatidylcholine (EPC) from Avanti Polar Lipids, Inc. (Alabaster, AL). The nAChR in asolectin is fully functional whereas in EPC membranes it may adopt a channel-inactive desensitized conformation (*25*, *26*).

FTIR Spectroscopy. FTIR spectra were acquired either on a Bio-Rad FTS-40 or on a Bio-Rad 40A spectrometer equipped with either a mercury cadmium telluride or deuterated triglycine sulfate detector for transmission and attenuated total reflectance (ATR) measurements, respectively. Each spectrometer was purged with dry air (dew point, 100 °C) from a separate Balston air-dryer (Haverhill, MA). All spectra were recorded at 2 cm^{-1} resolution. Spectral deconvolution was performed according to the method of Kauppinen et al. (*27*) with γ and resolution enhancement factors of 17.0 and 2.2, respectively. Prior to deconvolution, all spectra were stringently examined for the presence of water vapor using the mild spectral deconvolution procedure described previously (*28*).

$^1H/^2H$ Exchange. FTIR spectra were recorded during the time course of peptide $^1H/^2H$ exchange using the ATR technique. In each case, 250 μg of reconstituted nAChR protein was deposited on the surface of a germanium internal reflection element (Harrick, Ossining, NY). The bulk solvent was evaporated with a gentle stream of N_2 gas. After mounting the reflection element in an ATR liquid sample cell, each nAChR film was rehydrated with Torpedo Ringer buffer (250 mM NaCl, 5 mM KCl, 2 mM $MgCl_2$, 5 mM Na_2HPO_4, 3 mM $CaCl_2$, and 0.02% NaN_3). All spectra were recorded at 22.5 °C.

To monitor the spectral changes that occur over the first 12 h of peptide $^1H/^2H$ exchange, the nAChR membrane films were prepared in ^1H_2O buffer on a germanium internal reflection element as described above. After recording a quick 100-scan spectrum, the ^1H_2O buffer was replaced by ^2H_2O buffer, and infrared spectra with increasing numbers of scans (varying from 50 to 1500 scans/spectrum) were acquired over the next 12 h.

To record spectra under conditions of "extensive" peptide $^1H/^2H$ exchange, 250 μg nAChR protein aliquots were pelleted and resuspended twice in 2 mM phosphate, ^2H_2O buffer at pH 7.0 (pD 6.6) and then stored at 4 °C for 3 days (*24*). All pH values in ^2H_2O have been corrected according to the following: pH = pD + 0.4 (*49*). This leads to the exchange of roughly 75% of the peptide hydrogens. The samples were centrifuged, resuspended in fresh ^2H_2O buffer, and stored at −80 °C. The nAChR membranes were then deposited on the germanium internal reflection element as described above and rehydrated with ^2H_2O buffer at pH 7.0. After adjusting the buffer to the appropriate pH, spectra were recorded over the next 20 h (1500 scans/spectra, ∼1 h each) to exchange as much of the remaining 25% exchange-resistant peptide hydrogens as possible. Fifty millimolar CAPS was used to buffer the ^2H_2O solutions at elevated pH.

Thermal Denaturation Experiments. ^2H_2O nAChR samples (exposed to ^2H_2O for 3 days at pH 7.0, 4 °C, and then stored at −80 °C as described above) were centrifuged and resuspended in CAPS buffer at the noted pH before depositing on the surface of the CaF_2 window as described previously (*28*). Infrared spectra at the elevated pHs were recorded using a thermostatically controlled transmission cell. Spectra (256 scans) were typically recorded at 2−4 °C intervals between 25 and 75 °C. The nAChR was equilibrated for roughly 15 min at each temperature before data acquisition. The melting temperatures taken from the thermal denaturation curves are reported as the mean ± standard error and represent the average of three experiments except for the denaturation experiment at pH 11.0 for the nAChR in asolectin which is the average of two experiments and is reported as mean ± range.

RESULTS

FTIR spectra recorded over the first 12 h after exposure of affinity-purified nAChR reconstituted in soybean asolectin membranes to ^2H_2O buffer exhibit a number of spectral changes that reflect the exchange of peptide $N-^1H$ for $N-^2H$ (Figure 1A). The most noticeable is a dramatic decrease in

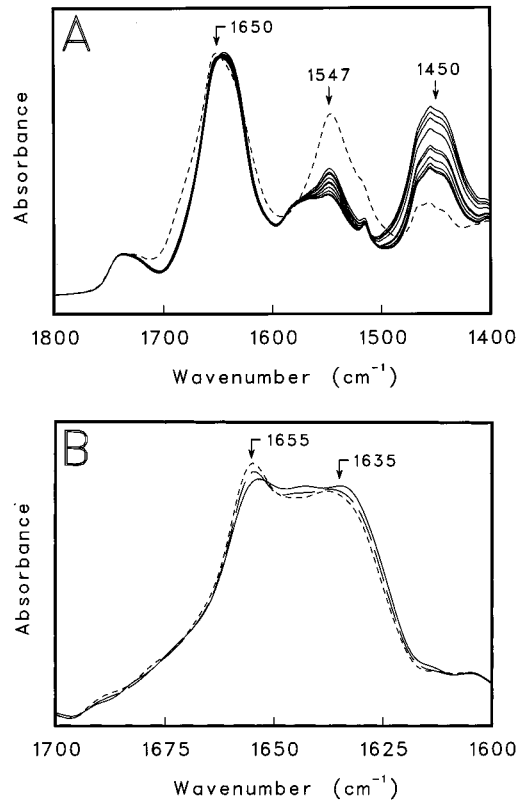

FIGURE 1: FTIR spectra of the nAChR in asolectin recorded in ^1H_2O buffer and as a function of time after exposure to ^2H_2O buffer. (A) The dashed line spectrum was recorded in ^1H_2O buffer. The solid line spectra were recorded from top to bottom at 1547 cm^{-1} after 6, 9, 12, 22, 50, 80, 170, 360, 600, and 780 min exposure to ^2H_2O. The spectral contribution of buffer in each spectrum was subtracted. (B) Resolution-enhanced amide I band from spectra recorded over the 1st, 3rd, and 12th h after exposure to ^2H_2O. Spectra are not scaled.

the intensity of the amide II band (primarily N$-^1$H bending) centered near 1547 cm^{-1}, which shifts down in frequency to 1450 cm^{-1} and provides a direct measure of both the time course and the extent of peptide $^1H/^2H$ exchange (see below). A quantitative analysis of the time-dependent amide II band shift shows that roughly 30% of the peptide hydrogens exchange within seconds of exposure of the nAChR to ^2H_2O, an additional 20% over the next 30 min, and an additional 10% over the next 12 h (*24*). The 30% rapidly exchanging peptide hydrogens likely exist in highly solvent-accessible random and turn conformations whereas those exchanging beyond this time frame must be involved in ordered secondary structures such as α-helix and *β*-sheet. Roughly 25% of the peptide hydrogens are resistant to exchange even after 3 days exposure of the nAChR to ^2H_2O at 4 °C. The 25% exchange-resistant peptide hydrogens likely include those found within the aqueous solvent-inaccessible regions of the lipid bilayer (see Discussion).

Exposure of the nAChR to ^2H_2O leads to subtle variations in the shape of the amide I band (primarily C═O stretch) located between 1600 and 1700 cm^{-1}. The frequency of the amide I vibration is sensitive to hydrogen bonding and thus both secondary structure and the exchange of peptide N$-^1$H for N$-^2$H. Changes in the amide I band shape observed upon initial exposure of the nAChR to ^2H_2O are likely the result of relatively large downshifts in the frequencies of the amide I component bands from the ∼30% highly solvent-accessible peptides that are involved in random and turn structures (*24*). In contrast, the exchange of peptide N$-^1$H for N$-^2$H over the 1−12 h time frame leads to relatively small downshifts in the frequencies of both the α-helix and *β*-sheet amide I component bands. Resolution enhancement reveals two main amide I component bands centered near 1655 and 1635 cm^{-1} that are highly characteristic of α-helix and *β*-sheet, respectively (Figure 1B). The downshifts in frequency of the α-helix and *β*-sheet vibrations lead to a decrease in intensity near 1655 cm^{-1} and a broadening of the amide I band toward 1630 cm^{-1}, respectively. Similar downshifts in frequency have been observed for numerous proteins and assigned to the downshift of both α-helices and *β*-sheets (*40*−*45*). Note that the time course of these component band shifts suggests that *β*-sheet peptide hydrogens exchange on a more rapid time scale than those involved in α-helical secondary structures (*24*). The strong intensity remaining near 1655 cm^{-1} after both 12 h and 3 days exposure (see Figure 5) to ^2H_2O suggests the presence of a substantial number of exchange-resistant α-helical peptide hydrogens and thus a large number of transmembrane α-helices (see Discussion). The possible existence of exchange-resistant *β*-sheet cannot be ascertained directly from these spectra because distinct bands for either the protiated or the deuterated forms of the *β*-sheet vibration are not resolved.

If nondenaturing conditions could be established for exchanging the ∼25% exchange-resistant peptide hydrogens in the nAChR, the ATR approach could be used to monitor any resulting downshifts in frequency of both α-helix and *β*-sheet amide I component bands and thus directly probe the secondary structure of the exchange-resistant peptide hydrogens (referred to as the exchange-resistant core). Typical physicochemical factors that enhance peptide $^1H/^2H$ exchange rates are elevated pH and temperature (*30*). Reconstitution of the nAChR into a more fluid lipid membrane such as EPC also accelerates peptide $^1H/^2H$ exchange (*29*). However, before testing the effects of these physicochemical factors on both the kinetics of peptide $^1H/^2H$ exchange and the resulting changes in the secondary structure sensitive amide I band, we first examined the effects of pH and membrane environment on the thermal stability of the nAChR. The latter was performed in order to establish nondenaturing alkaline conditions for the enhanced $^1H/^2H$ exchange.

Thermal Denaturation. The nAChR was preexposed to ^2H_2O buffer for 3 days at 4 °C (see Materials and Methods), and then spectra were recorded with increasing temperature as shown in Figure 2. The resulting spectra exhibit a number of changes in the amide I band shape including a decrease in amide I band intensity in the 1660−1630 cm^{-1} region coupled with the appearance of two new bands centered near 1680 and 1620 cm^{-1} that are highly characteristic of protein denaturation (*31*, *32*). A quantitative analysis of the increase in intensity near 1620 cm^{-1} that occurs as a function of increasing temperature reveals a sigmoidal melting curve with a melting temperature, T_m, for the nAChR in asolectin at pH 7.0 of 57.3 ± 1.1 °C (Figure 3). This value is similar to the T_m of ∼59 °C reported using both differential scanning calorimetry and FTIR for the nAChR in native membranes (*33*, *31*).

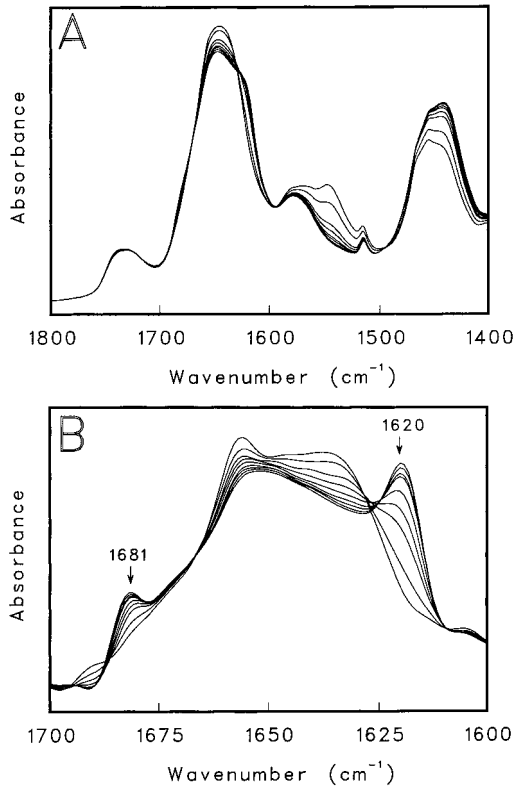

FIGURE 2: Thermal denaturation FTIR spectra of the nAChR in asolectin at pH 7.0 in ^2H_2O. The nAChR was exposed to ^2H_2O at pH 7.0, 4 °C, for 3 days (see Materials and Methods) and then resuspended at the noted pH. (A) An FTIR spectrum was recorded roughly every 30 min with temperature increments of 3−4 °C from 44 to 81 °C (from top to bottom at 1650 cm^{-1}). (B) Same as in (A) after resolution enhancement. Spectra are not scaled.

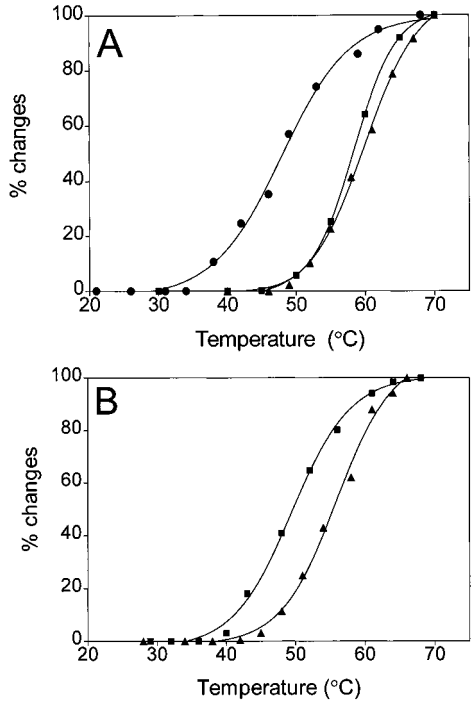

FIGURE 3: Thermal denaturation of the nAChR plotted as the percentage change in intensity at 1620 cm^{-1} versus increasing temperature. (A) nAChR in asolectin at pH 7.0 (▲), pH 9.0 (■) and pH 11.0 (●). (B) nAChR in EPC at pH 7.0 (▲) and pH 9.0 (■).

At pH 9.0, the measured T_m is 58.1 ± 1.6 °C for the nAChR in asolectin and is comparable to that observed at pH 7.0, indicating that this elevated pH has no detectable effect on the thermal stability of the nAChR. In contrast, at pH 10.0 (data not shown) and above, the temperature-induced spectral changes occur at increasingly lower temperatures (T_m is 49.9 ± 2.0 °C for the nAChR in asolectin at pH 11.0). A slight increase in intensity near both 1680 and 1620 cm^{-1} is also observed in the initial spectra recorded at the start of the denaturation experiments above pH 10.0. The appearance of these spectral features suggests that exposure of the nAChR in asolectin to buffer at pH 10 and above leads to the denaturation of a small percentage of each nAChR sample at room temperature. Further studies of the peptide $^1H/^2H$ exchange at pH > 10 were only performed for comparison with studies performed under "nondenaturing" conditions (see below).

The nAChR reconstituted into EPC membranes lacking cholesterol and anionic lipids is less thermally stable than the nAChR reconstituted into membranes composed of asolectin. Although the nAChR in both membranes have comparable T_m's at pH 7 (55.3 ± 0.4 °C in EPC), the T_m for the nAChR in EPC at pH 9.0 (47.2 ± 2.2 °C) is much lower than that observed for the nAChR in asolectin at pH 9 (Figure 3B). The initial spectra of the nAChR in EPC at pH 9.0 recorded at the start of the thermal denaturation experiments do not exhibit any spectral features indicative of denaturation, suggesting that the nAChR initially retains a native secondary structure at 22.5 °C. In contrast, the initial spectrum recorded at room temperature for the nAChR in EPC at higher values of pH exhibits bands near 1680 and 1620 cm^{-1} that are characteristic of a denatured nAChR. The shape of the amide I band in spectra recorded at elevated pHs is also relatively insensitive to increasing temperature, suggesting that a substantial portion of the nAChR is already in a denatured state at 22.5 °C.

Note that denaturation-induced changes in the amide I band shape can be distinguished from those that occur as a result of the $^1H/^2H$ exchange of peptides involved in α-helix and β-sheet. The $^1H/^2H$ exchange of neither α-helix nor β-sheet leads to the increased intensity of the denaturation-sensitive band near 1680 cm^{-1} (compare Figures 1B and 2B). The frequency of the denaturation-induced increase in intensity near 1620 cm^{-1} is also substantially lower than the 1630 cm^{-1} frequency at which there is an increase in intensity as a result of the $^1H/^2H$ exchange-induced downshift in the main β-sheet component band.

Extent of Peptide $^1H/^2H$ Exchange at Alkaline pH. The effects of elevated pH and membrane environment on the $^1H/^2H$ exchange kinetics were monitored for the nAChR under conditions where the receptor retains its native secondary structure (pH 7 and 9 in soybean asolectin and pH 9 in EPC) as well as under conditions where a small percentage of the receptor is initially in a denatured state at room temperature (pH 11 in asolectin). In each case, the AChR was preincubated for 3 days in ^2H_2O buffer at 4 °C, pH 7.0, to exchange the bulk (∼75%) of the peptide hydrogens for deuterium. The nAChR was then depositied on a germanium internal reflection crystal and exposed to ^2H_2O buffer at the designated alkaline pH to effect further exchange of the exchange-resistant core. Both the residual amide II band intensity and the spectral changes in the amide I band (see below) were monitored over the next 20 h. At

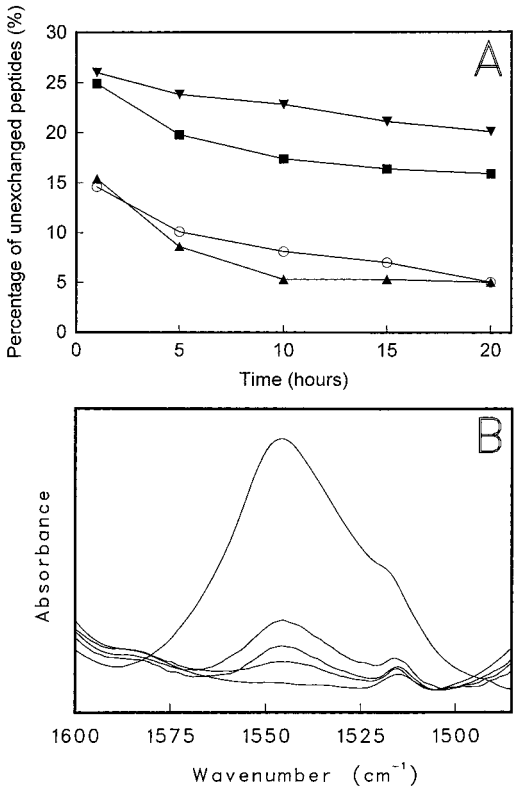

FIGURE 4: Effect of pH and membrane lipid environment on the $^1H/^2H$ exchange of those peptides located in the exchange-resistant core. The nAChR was exposed to ^2H_2O at neutral pH, 4 °C, for 3 days to exchange roughly 75% of the peptides N−^{1}H for N−^{2}H. The exchange kinetics of the remaining 25% N−^{1}H were then monitored over the subsequent 20 h at 22.5 °C at the designated pH. (A) Percentage of unexchanged peptides as a function of time after exposure to alkaline pH at 22.5 °C. nAChR/asolectin, pH 7.0 (▼), pH 9.0 (■), pH 11.0 (▲); and nAChR/EPC, pH 9.0 (○). Each curve represents the average of two experiments. (B) The amide II region in spectra of the nAChR recorded at pH 2.0 (see text). Top spectrum at 1547 cm^{-1} is the nAChR/asolectin in ^1H_2O buffer (after buffer subtraction). The remaining spectra from top to bottom at 1547 cm^{-1} are nAChR/asolectin in ^2H_2O buffer, pH 7.0, after 3 days at 4 °C; nAChR/asolectin after 3 days at pH 7.0, 4 °C, followed by pH 9.0 for 20 h at 22.5 °C; nAChR/EPC after 3 days at pH 7.0, 4 °C, followed by pH 9.0 for 20 h at 22.5 °C; and nAChR/asolectin after 3 days at pH 7.0, 4 °C, followed by pH 11.0 for 1 h at 95 °C to completely denature the protein.

the end of each experiment, the nAChR film was exposed to ^2H_2O buffer at pH 2.0 in order to shift the ionized Asp and Glu vibrations from near 1580 cm^{-1} up to the 1700−1740 cm^{-1} region (characteristic of the protiated form) and thus provide an unobstructed view of residual amide II band intensity (Figure 4B). The calculation of the percent unexchanged peptide hydrogens is discussed in detail elsewhere (*24*).

In all cases, alkaline pH led to an increase in both the rate and extent of exchange for the peptide hydrogens in the exchange-resistant core. At a given pH, the nAChR in EPC always exchanged to a greater extent than the nAChR in asolectin, consistent with the lower thermal stability of the receptor in this membrane environment. The greatest enhancement in the level of peptide $^1H/^2H$ exchange under nondenaturing conditions was found at pH 9 for the nAChR in EPC (also, see below). Roughly 5% of the total number of peptide hydrogens remained unexchanged for deuterium after the 20 h incubation period. This corresponds to an

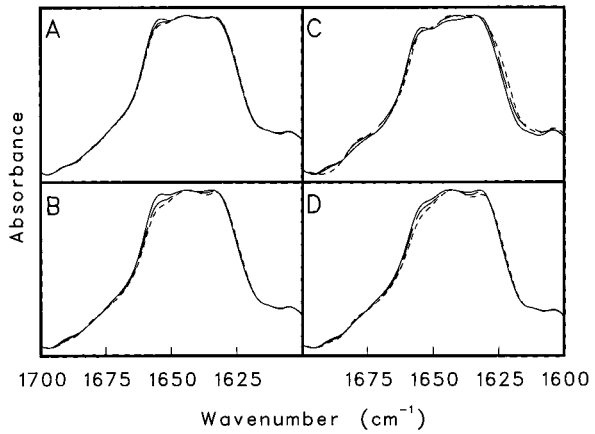

FIGURE 5: Resolution-enhanced amide I band in FTIR spectra of the nAChR recorded under conditions of alkaline-enhanced peptide $^1H/^2H$ exchange. The nAChR was first incubated for 3 days at 4 °C, in ^2H_2O buffer at pH 7.0; FTIR spectra were then recorded over the subsequent 20 h after exposure to ^2H_2O at the designated pH. Spectra of the nAChR in asolectin (panels A−C) and in EPC (D) were recorded at (A) pH 7.0, (B) pH 9.0, (C) pH 11.0, and (D) pH 9.0. Spectra in solid, long dash, and short dash lines, respectively, were recorded in (A) after 1, 10, and 20 h, in (B) after 1, 5, and 20 h, in (C) after 1, 3, and 20 h, and in (D) after 1, 3, and 20 h of ^2H_2O buffer exposure.

enhanced exchange of roughly 80% of the normally 25% exchange-resistant peptide hydrogens after 20 h. Increased temperatures also enhance the extent of $^1H/^2H$ exchange in the nAChR; however, temperatures above 22.5 °C were not studied due to the increased thermal instability of the nAChR at alkaline pH.

Effects of Enhanced Peptide $^1H/^2H$ Exchange on the Amide I Band. As shown in Figure 5, the $^1H/^2H$ exchange of the peptide hydrogens that are normally found in the exchange-resistant core under nondenaturing conditions (pH 7.0 and 9.0 for the nAChR in asolectin and pH 9.0 for the nAChR in EPC; also, see below) all exhibit similar variations in amide I band shape. The changes in band shape result predominantly from a decrease in intensity near 1655 cm^{-1} concomitant with an increase in intensity between 1640 and 1650 cm^{-1}. As discussed above, the loss in intensity at 1655 cm^{-1} is due to a downshift in frequency of the α-helical amide I component band and confirms that there are a large number of exchange-resistant α-helical peptide hydrogens in the nAChR. In contrast, there appears to be essentially no broadening near 1630 cm^{-1} that can be unequivocally attributed to the downshifts in frequency and thus $^1H/^2H$ exchange of exchange-resistant β-sheet (see below). Note that all three samples retain some unexchanged peptide hydrogens (minimum of ∼5% for the nAChR in EPC at pH 9.0). All three sets of spectra also exhibit residual amide I band intensity near 1655 cm^{-1} that is likely due to unexchanged α-helical peptides. Both the substantial downshifts in frequency of the α-helical amide I component band and the observation of a residual amide I component band reflecting unexchanged α-helical peptide hydrogens suggest that the vast majority of the exchange-resistant peptides in the nAChR exist in an α-helical conformation.

Note that the spectra presented in Figure 5 were all normalized to maximize their intensity in each panel. The normalization was performed because some of the spectra recorded at elevated pHs exhibit a slight decrease in amide

I band intensity over the time course of the experiment, possibly due to subtle effects of alkaline pH on the lipid bilayer. The substantial downshifts in frequency of α-helical amide I component bands upon enhanced peptide $^1H/^2H$ exchange are evident regardless of the scaling of the amide I bands. In contrast, it is difficult to unequivocally assess the occurrence of subtle downshifts in frequency of the β-sheet amide I component bands in the 1635−1630 cm^{-1} region because the detection of broadening near 1630 cm^{-1} depends on the scaling of the amide I band. In addition, exposure of the nAChR in EPC membranes to ^2H_2O at pH 9.0, 22.5 °C, eventually leads to an increase in intensity near both 1680 and 1620 cm^{-1}, suggesting a slight amount of protein denaturation. Difference spectra suggest that any changes that may occur in the 1635−1630 cm^{-1} region with enhanced peptide $^1H/^2H$ exchange are due to the increased intensity centered near 1620 cm^{-1} and thus denaturation of the nAChR. While we cannot unequivocally state that there are no exchange-resistant β-strands, our data suggest that β-strands represent a very small proportion, if any, of the exchange-resistant core.

$^1H/^2H$ exchange spectra recorded from the nAChR in asolectin at pH 11, where a proportion of the sample is initially in a denatured state at room temperature, exhibit pronounced spectral changes suggestive of nAChR denaturation (Figure 5C). The denaturation of the nAChR in asolectin at pH 11 occurs *without* a comparable decrease in intensity of the protiated α-helical component band at 1655 cm^{-1}, confirming that the spectral changes are due to denaturation of the nAChR and suggesting that the exchange-resistant peptides and thus likely the transmembrane domain are more resistant to denaturation than the extracellular domains. The data obtained at pH 11 and to a lesser extent at pH 9 (nAChR in EPC) also suggest that there is a kinetic component to the protein denaturation pathway (see *46* and references cited therein).

DISCUSSION

The goal of this work was to probe the secondary structure of the exchange-resistant core from the nAChR using a novel combination of FTIR and peptide $^1H/^2H$ exchange. Our data show that ∼25% of the nAChR peptide hydrogens are resistant to exchange after 3 days exposure to ^2H_2O at 4 °C. Most of the ∼25% nAChR peptide hydrogens can be exchanged for deuterium at room temperature under nondenaturing alkaline conditions. FTIR spectra of the nAChR recorded under these enhanced exchange conditions exhibit a downshift in frequency of the α-helical amide I component band whereas comparable downshifts in frequency of β-sheet component bands are absent. We have interpreted these spectral changes in terms of the existence of a large population of exchange-resistant α-helices that likely reside within the transmembrane domain. In contrast, the lack of band shifts that can be attributed unequivocally to the presence of exchange-resistant β-strands suggests an absence of transmembrane β-sheet.

The interpretation of our data in terms of the secondary structure of the transmembrane domain of the nAChR relies on two important assertions. First, it is assumed that the ∼25% exchange-resistant core *includes* those peptide hydrogens that reside within the transmembrane domain. This assumption is based on the fact that the aqueous solvent accessibility to the hydrophobic environment of the lipid bilayer is relatively low and thus should retard the $^1H/^2H$ exchange rates of the transmembrane peptide hydrogens. The transient folding/unfolding motions of ordered secondary structures that are necessary for rapid exchange may be restricted in transmembrane structures because such motions would expose the highly polar peptide N−H and C═O groups to the hydrophobic lipid acyl chains. These transient motions may be particularly restricted for the nAChR because relatively static transmembrane structures are likely required to ensure that the nAChR cation channel remains consistently closed in the absence of bound agonist.

The solvent inaccessibility of transmembrane peptide hydrogens in general has been shown experimentally in several studies of membrane protein hydrogen exchange kinetics (for a review, see *34*). A large percentage of exchange-resistant peptide hydrogens that appears to be related to the number of peptides found within the hydrophobic core of the lipid bilayer has been observed for the two integral membrane proteins rhodopsin and bacteriorhodopsin (*35*−*38*). An unusually large number of exchange-resistant peptides have been reported for the multisubunit photosynthetic reaction center (*46*). Even the transmembrane β-barrel pore, porin, exhibits a large number of exchange-resistant peptide hydrogens (*39*). For the nAChR, the roughly ∼25% peptide hydrogens that are resistant to exchange after 3 days exposure to ^2H_2O at 4 °C are estimated to be accurate within ±10% (for details, see ref *24*). This value is similar to the 20−25% of peptides predicted by hydrophobicity plots to exist within the membrane (*3*, *4*) and the 25−30% of the nAChR found within the lipid bilayer by both electron microscopy (*15*) and proteinase K digestion of the extramembranous portions of the nAChR (*21*). Although we cannot attribute the ∼25% exchange-resistant peptides in the nAChR exclusively to the transmembrane domains, it seems highly likely that the exchange-resistant core includes those peptides found in the transmembrane segments M1−M4.

The second major assertion of our experimental approach is that downshifts in frequency of α-helix and β-sheet amide I component bands upon peptide $^1H/^2H$ exchange can be specifically detected in infrared spectra using resolution enhancement techniques. We have shown previously that "relatively" large changes in the shape of the amide I band occur within seconds of exposure of the nAChR to ^2H_2O. These rapid spectral changes likely arise from the downshifts in frequency of roughly 30% of the total peptide carbonyls that are involved in highly solvent-accessible structures such as random coil and turns (*24*). In contrast, roughly 70% of the nAChR peptide hydrogens exchange over the minutes to hours and days or longer time frame. Since between 60 and 70% of the nAChR peptide hydrogens are involved in α-helix and β-sheet secondary structures (*47* and references cited therein), the relatively small changes that occur in the amide I band over the minutes to days time frame must result to a large extent from the downshifts in frequency of α-helix and β-sheet amide I component bands upon peptide $^1H/^2H$ exchange.

Note that the decrease in intensity near 1655 cm^{-1} and broadening of the amide I band near 1630 cm^{-1} over the *1*−*12 h time frame* after initial exposure of the nAChR to

^2H_2O occur with differing kinetics (*24*), indicating that these two spectral changes result from the exchange of peptides in two distinct types of secondary structures. This assertion is confirmed by the decrease in intensity near 1655 cm^{-1} that is observed in the absence of broadening toward 1630 cm^{-1} under the enhanced exchange conditions reported here. Infrared bands centered near 1655 and 1635 cm^{-1} are highly characteristic of α-helical and *β*-sheet secondary structures (*48*). The loss of intensity centered near 1655 cm^{-1} and the broadening of the amide I band near 1630 cm^{-1} are typical of the spectral changes detected for other proteins upon exposure to ^2H_2O (*40*−*44*) and which have been attributed to the downshifts in frequency of α-helix and *β*-sheet amide I component bands, respectively.

To accurately detect these subtle changes in the amide I band, the spectra must be recorded under highly stable conditions of temperature, pH, etc. The ATR technique is particularly advantageous for such measurements because the nAChR films on the germanium internal reflection element are relatively stable. A constant temperature in the ATR cell can easily be maintained. The buffer compartment surrounding the nAChR is also tightly sealed which limits any $^1H/^2H$ exchange between the ^2H_2O solvent and residual water vapor in the FTIR spectrometer. We also purge the spectrometer extensively before data acquisition and then stringently examine the resulting spectra for the presence of water vapor using the procedure described previously (*28*). Even the presence of very weak water vapor bands that are unobservable in the absorbance spectra can distort the spectra upon resolution enhancement to a point that uninterpretable changes in the amide I band upon peptide $^1H/^2H$ exchange would be observed (*28*).

Our data add to an increasingly large body of evidence which suggests an essentially α-helical secondary structure for the transmembrane segments M1−M4. Evidence in support of transmembrane α-helical secondary structures comes from biochemical studies using site-directed mutagenesis and photoaffinity labeling experiments (*11*−*14*). Spectroscopic analyses of both synthetic and proteolytically generated transmembrane polypeptides are also consistent with an α-helical secondary structure for M1−M4, although M1 likely forms a distorted α-helix due to the presence of proline residues (*16*, *17*, *20*).

In contrast, FTIR spectra of nAChR treated with proteinase-K to remove the extramembranous domains exhibit bands at frequencies normally assigned to *β*-sheet (*21*). While these data are highly suggestive of transmembrane *β*-strands, prolonged proteolytic treatment may lead to detrimental structural consequences to the transmembrane domains. In addition, it is not generally possible to completely remove all the extramembranous peptides from integral membrane proteins using proteolytic treatment. With affinity-purified nAChR membranes, we have been unable to reproduce the extensive proteolysis reported by Görne-Tschelnokow et al. (1994) even under harsh proteolytic conditions (Méthot and Baenziger, unpublished observations). The reported secondary structures may therefore not pertain exclusively to the transmembrane segments.

While the hydrogen/deuterium exchange approach used here cannot provide a quantitative assessment of the secondary structural content of integral membrane protein transmembrane domains in general, all experiments were performed on intact nAChR, and thus the analysis does not suffer from the potentially harmful structural effects of proteolytic degradation. Given the importance of structural analyses of the transmembrane domains of integral membrane proteins in general, this FTIR and hydrogen/deuterium approach provides a complementary method for probing the secondary structures of membrane protein transmembrane domains.

Finally, an interesting feature of this work is the obervation that the membrane environment affects both the hydrogen exchange kinetics and the stability of the nAChR under alkaline conditions. The ability of altered membrane physical properties to modulate the internal dynamics of the nAChR could provide a mechanism whereby lipids modulate membrane protein function.

REFERENCES

1. Pradier, L., and McNamee, M. G. (1992) in *The Structure of Biological Membranes* (Yeagle, P. L., Ed.) pp 1047−1106, CRC Press, Boca Raton, FL.
2. Hucho, F., Tsetlin, V. I., and Machold, J. (1996) *Eur. J. Biochem. 239*, 539−557.
3. Noda, M., Takahashi, H., Tanabe, T., Toyosato, M., Kikyotani, S., Furutani, Y., Hirose, T., Takashima, H., Inayama, S., Miyata, T., and Numa, S. (1983) *Nature 302*, 528−532.
4. Claudio, T., Balliver, M., Patrick, J., and Heinemann, S. (1983) *Proc. Natl. Acad. Sci. U.S.A. 80*, 1111−1115.
5. Leonard, R. J., Labarca, C. G., Charnet, P., Davidson, N., and Lester, H. A. (1988) *Nature 242*, 1578−1581.
6. Imoto, K., Busch, C., Sakmann, B., Mishina, M., Konno, T., Nakai, J., Bujo, H., Mori, Y., Fukuda, K., and Numa, S. (1988) *Nature 335*, 645−648.
7. Tobimatsu, T., Fujita, Y., Fukada, K., Tanaka, K.-I., Mori, Y., Konno, T., Mishina, M., and Numa, S. (1987) *FEBS Lett. 222*, 56−62.
8. Lasalde, J. A., Tamamizu, S., Butler, D. H., Vibat, C. R. T., Hung, B., and McNamee, M. G. (1996) *Biochemistry 35*, 14139−14148.
9. Campos-Caro, A., Rovira, J. C., Vincente-Agulló, F., Ballesta, J. J., Sala, S., Criado, M., and Sala, F. (1997) *Biochemistry 36*, 2709−2715.
10. Henderson, R. (1975) *J. Mol. Biol. 93*, 123−138.
11. Giraudat, J., Dennis, M., Heidmann, T. H., Maumont, P. Y., Lederer, F., and Changeux, J.-P. (1987) *Biochemistry 26*, 2410−2418.
12. Charnet, P., Labarca, C., Leonard, R. J., Vogelaar, N. J., Czyzyk, L., Gouin, A., Davidson, N., and Lester, H. A. (1990) *Neuron 4*, 87−95.
13. Revah, F., Bertrand, D., Glazi, J.-L., Devillers-Thiéry, A., Mulle, C., Hussy, N., Bertrand, S., Ballivet, M., and Changeux, J.-P. (1990) *Nature 353*, 846−849.
14. White, B. H., and Cohen, J. B. (1992) *J. Biol. Chem. 267*, 15770−15783.
15. Unwin, N. (1993) *J. Mol. Biol. 229*, 1101−1124.
16. Montal, M., Montal, M. S., and Tomich, J. M. (1990) *Proc. Natl. Acad. Sci. U.S.A. 87*, 6929−6933.
17. Bechinger, B., Kim, Y., Chirlian, L. E., Gesell, J., Neumann, J., Montal, M., Tomich, J., Zasloff, M., and Opella, S. J. (1991) *J. Biomol. NMR 1*, 167−173.
18. Blanton, M. P., and Cohen, J. B. (1992) *Biochemistry 31*, 3738−3750.
19. Blanton, M. P., and Cohen, J. B. (1994) *Biochemistry 33*, 2859−2872.
20. Corbin, J., Méthot, N., Wang, H. H., Baenziger, J. E., and Blanton, M. P. (1998) *J. Biol. Chem. 273*, 771−777.
21. Görne-Tschelnokow, U., Strecker, A., Kaduk, C., Naumann, D., and Hucho, F. (1994) *EMBO J. 13*, 338−341.
22. Ortells, M. O., and Lunt, G. G. (1996) *Protein Eng. 9*, 51−59.
23. Unwin, N. (1995) *Nature 373*, 37−43.

24. Baenziger, J. E., and Méthot, N. (1995) *J. Biol. Chem. 270*, 29129−29137.
25. McCarthy, M. P., and Moore, M. A. (1992*) J. Biol. Chem. 267*, 7655−7663.
26. Ryan, S. E., Demers, C. N., Chew, J. P., and Baenziger, J. E. (1996) *J. Biol. Chem. 271*, 24590−24597.
27. Kauppinen, J. K., Moffat, D. J., Mantsch, H. H., and Cameron, D. G. (1981) *Appl. Spectrosc. 35*, 271−276.
28. Reid, S. E., Moffatt, D. J., and Baenziger, J. E. (1996) *Spectrochim. Acta 52*, 1347−1356.
29. Méthot, N., Demers, C. N., and Baenziger, J. E. (1995) *Biochemistry 34*, 15142−15149.
30. Englander, S. W., Downer, N. W., and Teitelbaum, H. (1972) *Annu. Rev. Biochem. 41*, 903−924.
31. Ferandez-Ballester, G., Castresana, J., Arrondo, J.-L. R., Ferragut, J. A., and Gonzalez-Ros, J. M.(1992) *Biochem. J. 288*, 421−426.
32. Knöle, R., and Hübner, W. (1995) *Biochemistry 34*, 10970−10975.
33. Artigues, A., Villar, M. T., Ferragut, J. A., and Gonzalez-Ros, J. M. (1987) *Arch. Biochem. Biophys. 258*, 33−41.
34. Goormaghtigh, E., Cabiaux, V., and Ruysschaert, J.-M. (1994) *Subcell. Biochem. 23*, 409−420.
35. Earnest, T. N., Herzfeld, J., and Rothschild, K. J. (1990) *Biophys. J 58*, 1539−1546.
36. Downer, N. W., Bruchman, T. J., and Hazzard, J. H. (1986) *J. Biol. Chem. 261*, 3640−3647.
37. Haris, P. I., Coke, M., and Chapman, D. (1989) *Biochim. Biophys. Acta 995*, 160−167.
38. Konishi, T., and Packer, L. (1977) *FEBS Lett. 80*, 455−458.
39. Kleffel, B., Garavito, R. M., Baumeister, W., and Rosenbusch, J. P. (1985) *EMBO J. 4*, 903−924.
40. Susi, H., Timasheff, S. N., and Stevens, L. (1967) *J. Biol. Chem. 242*, 5460−5466.
41. Olinger, J. M., Hill, D. M., Jakobsen, R. J., and Brody, R. S. (1986) *Biochim. Biophys. Acta 869*, 89−98.
42. Haris, P. I., Lee D. C., and Chapman, D. (1986) *Biochim. Biophys. Acta 874*, 255−265.
43. Baenziger, J. E., and Chew, J. P. (1997) *Biochemistry 36*, 3617−3624.
44. Heimburg, T., and Marsh, D. (1993) *Biophys. J 65*, 2408−2417.
45. Davoodi, J., Wakarchuk, W. W., Campbell, R. L., Carey, P. R., and Surewicz, W. K. (1995) *Eur. J. Biochem. 232*, 839−843.
46. Nabedryk, E., Andrianambinintsoa, S., Mäntele, W., and Breton, J. (1988) *NATO ASI Ser., Ser. A 168*, 237−250.
47. Méthot, N., McCarthy, M. P., and Baenziger, J. E. (1994) *Biochemistry 33*, 7709−7717.
48. Jackson, M., and Mantsch, H. H. (1995) *Crit. Rev. Biochem. Mol. Biol. 30*, 95−120.
49. Glasoe, P. F., and Long, F. A. (1960) *J. Phys. Chem. 64*, 188−193.

BI980848O